The multicatalytic proteinase complex (proteasome): structure and conformational changes associated with changes in proteolytic activity

Hakim DJABALLAH,* Arthur J. ROWE,* Stephen E. HARDING† and A. Jennifer RIVETT*‡

*Department of Biochemistry, University of Leicester, Leicester LE1 7RH, U.K.,
and †Department of Applied Biochemistry and Food Science, University of Nottingham, Sutton Bonington LE12 5RD, U.K.

The multicatalytic proteinase complex or proteasome is a high-molecular-mass multisubunit proteinase which is found in the nucleus and cytoplasm of eukaryotic cells. Electron microscopy of negatively stained rat liver proteinase preparations suggests that the particle has a hollow cylindrical shape (approximate width 11 nm and height 17 nm using methylamine tungstate as the negative stain) with a pseudo-helical arrangement of subunits rather than the directly stacked arrangement suggested previously. The side-on view has a 2-fold rotational symmetry, while end-on there appears to be six or seven subunits around the ring. This model is very different from that proposed by others for the proteinase from rat liver but resembles the structure of the simpler archaebacterial proteasome. The possibility of conformational changes associated with the addition of effectors of proteolytic activity has been investigated by sedimentation velocity analysis and dynamic light-scattering measurements. The results provide the first direct evidence for conformational changes associated with the observed positive co-operativity in one component of the peptidylglutamylpeptide hydrolase activity as well as with the stimulation of peptidylglutamylpeptide hydrolase activities by $MnCl_2$. In the latter case, there appears to be a correlation between changes in the shape of the molecule and the effect on activity. KCl and low concentrations of SDS may also act by inducing conformational changes within the complex. Sedimentation-velocity measurements also provide evidence for the formation of intermediates during dissociation of the complex by urea, guanidinium chloride or sodium thiocyanate. Dissociation of the complex either by these agents or by treatment at low pH leads to inactivation of its proteolytic components. The results suggest that activation and inhibition of the various proteolytic activities may be mediated by measurable changes in size and shape of the molecules.

INTRODUCTION

The multicatalytic proteinase (MCP) or proteasome is a widely distributed high-molecular-mass intracellular proteinase. MCP has been implicated in non-lysosomal pathways of intracellular protein degradation including the ubiquitin-dependent pathway and, more recently, in antigen processing (see reviews: Orlowski, 1990; Rivett, 1993).

There are several discrepancies in the literature with regard to the structure of the mammalian MCP molecule. Molecular masses in the range of 500–850 kDa have been reported and $s_{20,w}$ values ranging from 16S to 22S (Harris, 1988: Rivett, 1989a). The many different types of subunit have molecular masses of 20–35 kDa (Orlowski, 1990; Rivett and Sweeney, 1991; Heinemeyer et al., 1991). The MCP purified from rat muscle was proposed to have a hollow cylindrical structure composed of a stack of four hexagonal rings based on electron microscopy and laser light-scattering data (Kopp et al., 1986), whereas the rat liver MCP has been suggested to be a disc-shaped molecule with 8-fold symmetry (Arrigo et al., 1988; Tanaka et al., 1988b). Results of later studies with the rat muscle MCP suggested a reel-shaped molecule lacking true 6-fold symmetry (Baumeister et al., 1988). More recently the structure of the closely related proteinase isolated from archaebacteria (Dahlmann et al., 1989) has been characterized in some detail (Pühler et al., 1992) and is believed to have 7-fold symmetry.

Eukaryotic MCPs have multiple proteolytic activities of different specificities (Rivett, 1989a; Orlowski, 1990). Activities catalysing cleavage of peptide bonds on the carboxyl side of basic, hydrophobic or acidic amino acid residues have been referred to as 'trypsin-like', 'chymotrypsin-like' and 'peptidylglutamylpeptide hydrolase' activities respectively (Wilk and Orlowski, 1983). They are believed to be catalysed at independent catalytic sites, of which it is now clear there are at least five (Djaballah et al., 1992; Cardozo et al., 1992; Yu et al., 1991). The peptidylglutamylpeptide hydrolase activity, which is sensitive to a variety of effectors, is catalysed by two distinct components, which will be referred to as LLE1 and LLE2 (Djaballah and Rivett, 1992). The LLE1 component has the higher affinity for the substrate Z-Leu-Leu-Glu-β-naphthylamide (LLE-NA). Activity of the LLE2 component shows a sigmoidal dependence on substrate concentration which can be interpreted as positive co-operativity (Djaballah and Rivett, 1992). It is not yet clear whether this phenomenon can be explained by the action of multiple equivalent sites within the complex or by allosteric activation. Low concentrations of SDS appear to act as an allosteric activator (Arribas and Castaño, 1990) and both LLE1 and LLE2 activities can be stimulated by Mn^{2+} ions (Djaballah and Rivett, 1992). KCl (50 mM), on the other hand, causes inhibition of LLE2 activity, but has little effect on LLE1.

The present study was undertaken not only to clarify the structure of the rat liver MCP, which has been communicated previously (Rivett et al., 1991), but also to investigate the possibility of conformational changes associated with the positive co-operativity and the effects of known activators of peptidylglutamylpeptide hydrolase activities as well as to investigate the strength of the subunit interactions within the complex.

Abbreviations used: AAF-AMC, Ala-Ala-Phe-7-amido-4-methylcoumarin; LLE-NA, Z-Leu-Leu-Glu-β-naphthylamide; LLVY-AMC, succinyl-Leu-Leu-Val-Tyr-7-amido-4-methylcoumarin; LSTR-AMC, *N*-tBoc-Leu-Ser-Thr-Arg-7-amido-4-methylcoumarin; MCP, multicatalytic proteinase (multicatalytic endopeptidase complex; EC 3.4.99.46).

‡ To whom correspondence should be addressed.

EXPERIMENTAL

Materials

Rats (Wistar) were obtained from the University of Leicester Biomedical Services Unit. LLE-NA, Ala-Ala-Phe-7-amido-4-methylcoumarin (AAF-AMC), Z-Leu-Leu-Val-Tyr-7-amido-4-methylcoumarin (LLVY-AMC), BSA and sodium thiocyanate were purchased from Sigma Chemical Co. *N*-tBoc-Leu-Ser-Thr-Arg-7-amido-4-methylcoumarin (LSTR-AMC) was purchased from the Peptide Institute. Guanidinium chloride and urea were of Aristar grade from BDH. All reagents were of analytical grade.

Purification of the proteinase

The purification of MCP was carried out from fresh rat livers as described previously (Rivett and Sweeney, 1991). The purified enzyme was stored at −20 °C in 50 mM potassium phosphate buffer, pH 7.0, containing 1 mM 2-mercaptoethanol, 0.1 mM EDTA and 10% (v/v) glycerol at a protein concentration of 1 mg/ml. Protein concentrations were determined by the method of Bradford (1976) using the reagent from Bio-Rad with BSA as standard, which gives a very good approximation to the actual protein concentration (Savory and Rivett, 1993).

Determination of proteinase activities

MCP activities were assayed by fluorimetric measurement of the release of 7-amino-4-methylcoumarin or β-naphthylamine after incubation with a synthetic peptide substrate. The substrates AAF-AMC (40 μM), LLVY-AMC (40 μM), LSTR-AMC (40 μM) and LLE-NA (0.1 or 0.4 mM) were chosen to assay five proteolytic activities of the complex (Djaballah et al., 1992). Assays containing 1–2 μg of proteinase and a substrate in 50 mM Hepes/KOH buffer, pH 7.5, were carried out at 37 °C for 20 or 30 min as described previously (Rivett, 1989b; Djaballah et al., 1992).

Electron microscopy

Negative staining of samples was carried out on copper grids covered with carbon film, which had been rendered hydrophilic by a 30 s exposure to glow discharge in a plasma cleaner. MCP preparations (0.01–0.2 mg/ml) were applied to a grid and the molecules were left to adsorb for 5 min. Samples were then stained with ammonium molybdate [2% (w/v), pH 7.0], methylamine tungstate [2% (w/v), pH 6.0], sodium phosphotungstate [2% (w/v), pH 6.8], uranyl acetate [2% (w/v), pH 4.2] or sodium tungstoborate [2% (w/v), pH 6.8], before being viewed in a Siemens Elmiskop 102 or a JEOl 100 CX electron microscope at a magnification of 100000× or 150000× with an acceleration voltage of 80 kV. The electron microscopes were calibrated using a calibration replica.

Sedimentation velocity

Sedimentation velocity analysis was carried out on either the MSE Centriscan-75 analytical ultracentrifuge or the Beckman XL-A analytical ultracentrifuge using scanning absorption optics at 280 nm. For samples containing LLE-NA, solute distributions were recorded at a wavelength of 295 nm instead of 278 nm in order to reduce the interference due to absorbance of the naphthylamide group. Proteinase samples in 50 mM Hepes/KOH, pH 7.5, containing 1 mM dithiothreitol, were loaded into cells, avoiding generation of shearing forces. The cells were placed in the rotor and centrifuged at 25000 rev./min at 20 °C. The sedimentation boundaries were recorded, for each sample, at fixed intervals (5–12 min). Sedimentation coefficients ($s_{20,w}$) were determined from the rate of migration of the midpoint of the sedimenting boundary for each time point and then these positions were digitized directly from the recorder traces using an Apple Graphics Tablet linked to an Apple II+ microcomputer. The program calculates the $s_{20,w}$ values corrected for rotor expansion, reference to reference calibration and true rotor speed (Bowen and Rowe, 1970); these values were then corrected to standard solvent conditions (water at 20 °C) in the standard way (see e.g. van Holde, 1985) to give $s_{20,w}$. Because of the low protein concentrations employed (0.4–0.8 mg/ml), concentration effects were assumed to be negligible.

Dynamic light scattering

The translational diffusion coefficient was measured by dynamic light-scattering techniques using a BIOTAGE model 801 molecular size detector. Photons that are scattered at 90° to the incident laser beam are counted and the time constant of intensity fluctuation is obtained by autocorrelation of these data (Claes et al., 1992). As above, protein concentration (0.1 mg/ml) effects were deemed negligible. Also the assumption was made that rotational diffusion effects were negligible (i.e. no correction was made for angular dependence of the autocorrelation function). The hydrodynamic radius (r_H) was calculated from the diffusion coefficient, D_T, using the Stokes–Einstein equation (Berne and Pecora, 1976):

$$D_T = kT/6\pi\eta r_H$$

where k = Boltzmann constant, T = absolute temperature and η = viscosity.

RESULTS

Size and shape of MCP determined by electron microscopy

Electron microscopy of negatively stained MCP preparations showed two types of image: a rectangular outline with four bands transverse to the longer axis, and an approximately circular ring-shaped outline, with a hollow centre (Figures 1a and 1b and 2a). Using uranyl acetate as the negative stain (Figure 2a), the outer diameter of the ring (12.4 nm) corresponds closely to the width of the rectangular images (11.7 nm), and the length of the rectangular images was 19.6 nm (Table 1). It therefore seems very highly probable that these two types of image are alternative views of the same structure as suggested previously (Baumeister et al., 1988). The 'end-on' view suggests that six or seven is the most probable number of subunits making the ring, and four of these rings appear to be stacked on top of each other. Breaks in the ring domain were not infrequently seen but it is unclear as to whether these correspond to a real feature.

MCP particles stained with methylamine tungstate were of somewhat greater overall regularity (Figure 1b), and the images seen, although of comparable overall dimensions, were a little less elongated at 16.8 nm, with a width for the rectangular images of 10.9 nm (Table 1). Optical transforms of individual particles show a pattern of some complexity (Figure 1c). The expected meridional reflection corresponding to the spacing of the four stacks was not observed but there was an intense reflection near to meridional at the second order and, with some observed particles, detail which is suggestive of helical organization. Detailed model building will be required to interpret these patterns fully.

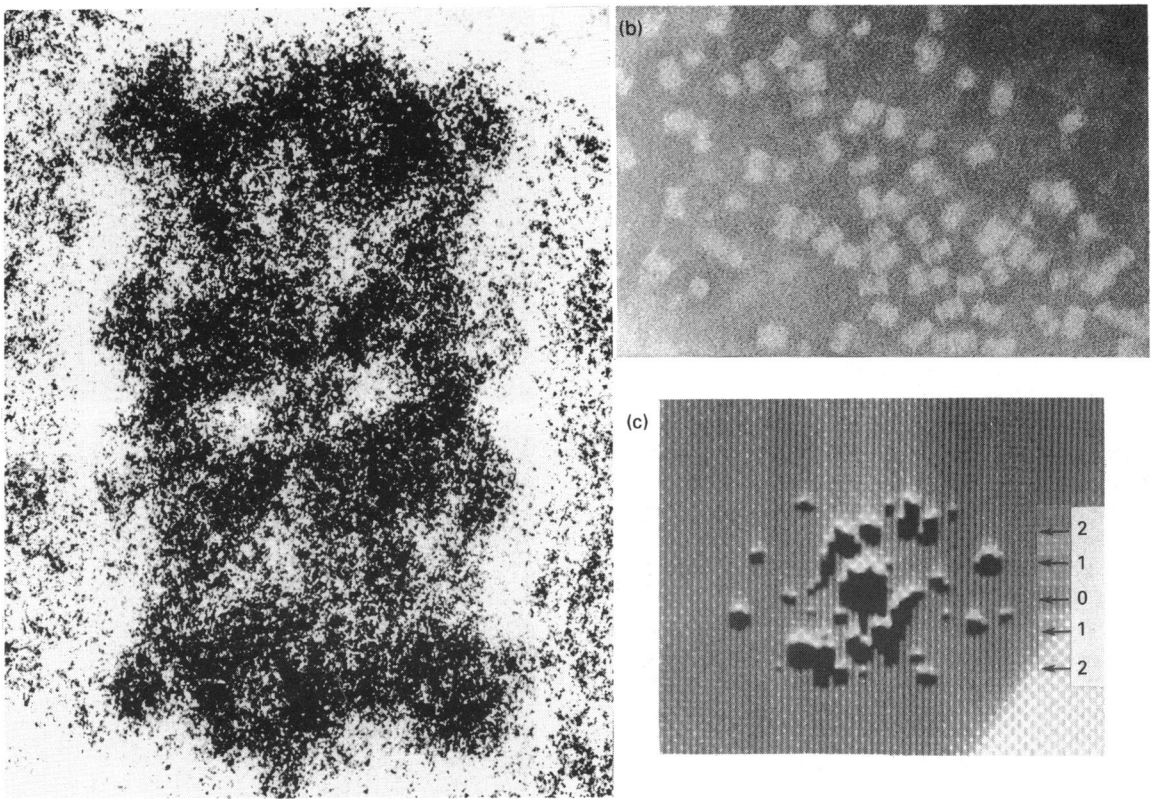

Figure 1 Electron microscopy of negatively stained rat liver MCP preparations

(**a**) Magnification (100000 ×) of a single MCP particle from (**b**) enlarged after contrast enhancement. (**b**) Electron micrograph of MCP particles negatively stained in methylamine tungstate. (**c**) An optical transform of a typical particle from (**a**). The latter was obtained using a Rank Taylor Hobson image analyser, an optical diffractometer with an on-line camera and analogue signal processing facilities: level control and a small degree of low-pass filtering were employed, and the scaling on the screen photographed was calibrated with a grating. Arrows indicate first- (1) and second- (2) order layer lines.

Conformational changes associated with activation by bivalent metal ions

The effect of $MnCl_2$ on the shape of the complex was investigated by electron microscopy of proteinase preparations containing $MnCl_2$, using uranyl acetate as the negative contrast medium (Figure 2). At a $MnCl_2$ concentration of 1 mM, the particles were found to adhere to the grid in larger numbers than in its absence, with some particles aggregating together in an end-to-end manner. It is not clear whether the aggregation is real or not (Figure 2b). There were more particles viewed end-on rather than side-on, with the disappearance of the hollow centre of most of them and the appearance of a raspberry-like shape as illustrated in Figure 2b. The above changes were also reflected by the increase in the size of the particles from an outer diameter of 12.4 nm to 14.8 nm, and from a length of 19.6 nm to 20.6 nm (Table 1). At 10 mM $MnCl_2$, damage and aggregation of particles was observed, leaving few remaining intact (Figures 2c and 2d). An increase in particles viewed side-on was observed, with some of them aggregating in an end-to-end manner. The outer diameter of the remaining control-like intact particles was reduced from 14.8 nm in the presence of 1 mM $MnCl_2$ to 13.1 nm in the presence of 10 mM $MnCl_2$ (Table 1).

A translational diffusion coefficient (D_T) of 2.78×10^{-7} cm^2/s was obtained for the control preparation of MCP. The presence of 1 mM $MnCl_2$ caused only about 1% change in D_T (2.76×10^{-7} cm^2/s), but 10 mM $MnCl_2$ caused a 50% drop in the D_T value from 2.78×10^{-7} cm^2/s to 1.35×10^{-7} cm^2/s. The hydrodynamic radius (r_H) of the complex was calculated to be 8.59 nm for preparations compared with an r_H of 8.53 nm in the presence of 1 mM $MnCl_2$ (Table 2). The inclusion of 1 mM $MnCl_2$ (or $CdCl_2$ or $MgCl_2$) reduced the sedimentation coefficient ($s_{20,w}$) of the proteinase (Table 3). In contrast, inclusion of the same concentration of either $ZnCl_2$ or $CdCl_2$ caused precipitation of the complex.

Correlation of conformational changes with changes in proteolytic activities was investigated by sedimentation-velocity measurements. As $MnCl_2$ concentration was increased to 1 mM, $s_{20,w}$ decreased from a value of 17.9S to a value of 14.0S in a more or less linear fashion. This parallelled an increase in activity of the non-co-operative component of the peptidylglutamylpeptide hydrolase activity (LLE1) by up to 3-fold stimulation (Figure 3a) and in that of the co-operative component (LLE2) by up to 2-fold (Figure 3b). Above 1 mM $MnCl_2$, the $s_{20,w}$ increased to a value of 17.6S at 10 mM $MnCl_2$, at which concentration it is inhibitory to both LLE1 and LLE2 activities (Figure 3).

Effects of high substrate concentration, SDS and KCl

LLE-NA, the synthetic substrate used to assay the peptidylglutamylpeptide hydrolase activity, had little effect on the sedimentation velocity when included at a concentration of 0.1 mM. However, with concentrations at which positive co-operativity is observed (e.g. 0.4 mM), an increase in the $s_{20,w}$ value from 17.7S to 19.7S was observed (Table 3).

The effects of several other effectors of peptidylglutamylpeptide

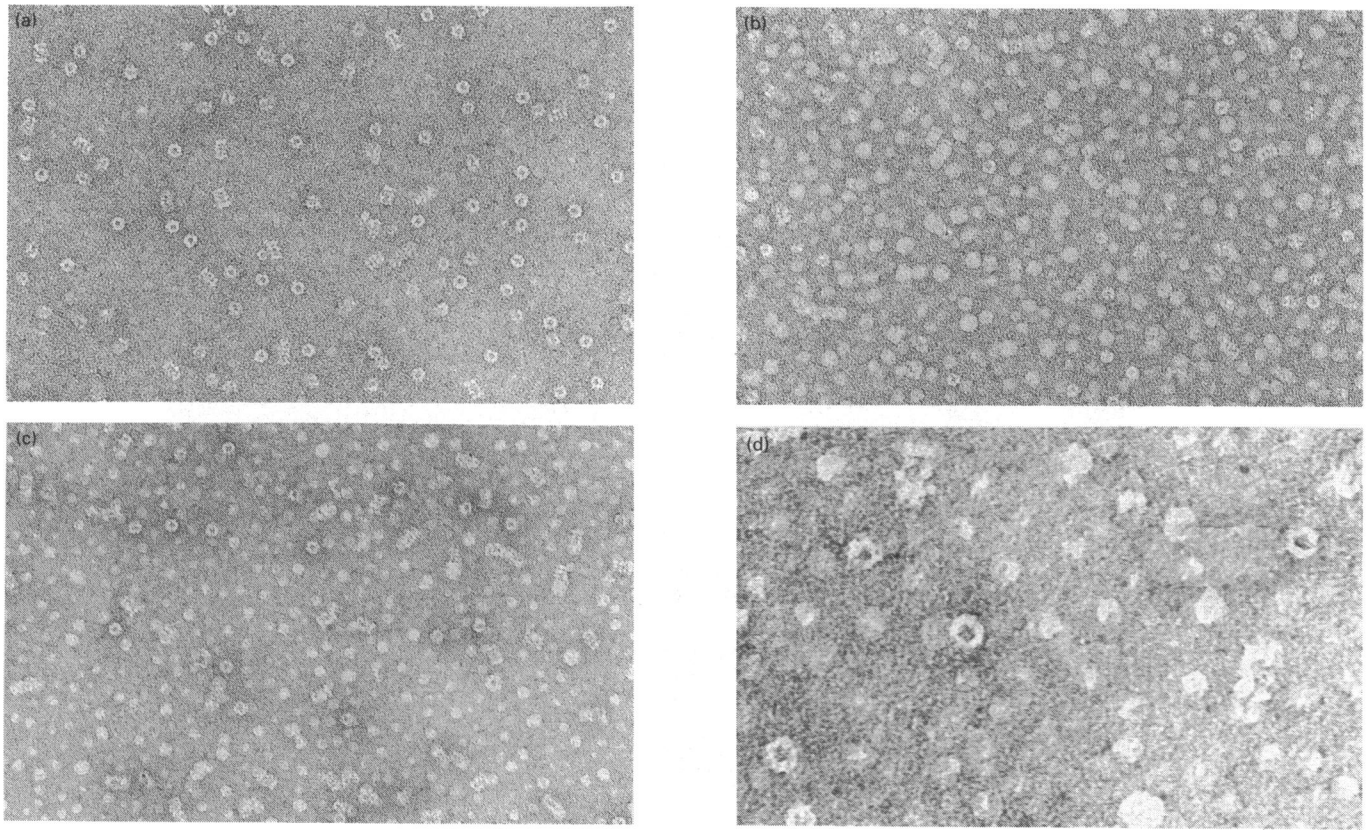

Figure 2 Electron microscopy of MCP particles negatively stained in uranyl acetate showing the effects of $MnCl_2$

Electron micrograph of MCP particles (**a**) in the absence of metal ions, (**b**) in the presence of 1 mM $MnCl_2$ and (**c**) in the presence of 10 mM $MnCl_2$. (**d**) Electron micrograph of MCP particles enlarged from (**c**). Magnification of 183000 × for (**a**), (**b**) and (**c**), and 250000 × for (**d**).

Table 1 Dimensions of the MCP complex obtained by electron microscopy

Values given are means ± S.E.M. for *n* molecules evaluated. Diameter = outer diameter of the molecule measured across the ring. Width = width determined from the side-on view of the molecule.

Treatment	Diameter (nm)	Width (nm)	Length (nm)	*n*
Control (methylamine tungstate)	10.91 ± 0.10	–	16.81 ± 0.10	114
Control (uranyl acetate)	12.42 ± 0.14	11.68 ± 0.22	19.61 ± 0.20	94
1 mM $MnCl_2$ (uranyl acetate)	14.83 ± 0.13	–	20.65 ± 0.93	273
10 mM $MnCl_2$ (uranyl acetate)	13.10 ± 0.34	–	–	70

Table 2 Physicochemical properties of the MCP complex

Property	Method of analysis	MCP	MCP + 1 mM $MnCl_2$
$M_{r,w}$	Sedimentation equilibrium	650000	–
	Sedimentation velocity and diffusion	575000 ± 37000	–
$s_{20,w}$	Sedimentation velocity	17.7 ± 0.2S	13.9 ± 0.2S
$10^7 \times D_T$ (cm^2/s)	Dynamic light scattering	2.78 ± 0.05	2.76 ± 0.10
Partial specific volume	From amino acid composition (Tanaka et al., 1986)	0.734 ml/g	–
r_H (nm)	From $M_{r,w}$ and $s_{20,w}$	8.70	–
	From D_T	8.59 ± 0.04	8.53 ± 0.20
	From electron microscopy	8.00 ± 0.17	8.87 ± 0.50

hydrolase activity on the conformation of the complex were also investigated by means of sedimentation-velocity analysis (Table 3). Addition of 50 mM KCl, an inhibitor of the co-operative LLE2 component (Djaballah and Rivett, 1992), caused a substantial decrease in sedimentation velocity to 13.9S (Table 3). The presence of a low concentration of SDS (0.01 %) caused an increase in the $s_{20,w}$ value from 17.7S to 21.2S, whereas a higher SDS concentration (0.02 %) decreased the sedimentation velocity but also showed evidence of some dissociation of the complex as well as of some aggregated material. Exposing the proteinase to 65 °C for 5 min caused a slight decrease in the $s_{20,w}$ value.

Dissociation of the complex

Adjusting the pH of the proteinase solution with 1 M glycine/HCl to pH 2.3 and with 1 M glycine/NaOH to pH 11.5 resulted in

Table 3 Sedimentation velocity of the MCP complex in the presence of effectors of peptidylglutamylpeptide hydrolase activity

Determinations of $s_{20,w}$ values were carried out using a Centriscan 75 as described in the Experimental section.

Treatment	Concentration	Effect on activity	$s_{20,w}$
Control	–		17.7±0.2
$MnCl_2$	(1 mM)	Stimulation of LLE1 and LLE2	13.9±0.2
$CaCl_2$	(1 mM)		15.5±0.1
$MgCl_2$	(1 mM)		16.7±0.1
KCl	(50 mM)	Inhibition of LLE2	13.9±0.2
SDS	(0.01%)	Stimulation of LLE1 and LLE2	21.2±0.2
SDS	(0.02%)		15.5±0.6
LLE-NA	(0.1 mM)	Below concentration at which positive co-operativity is observed	17.3±0.5
LLE-NA	(0.4 mM)	Co-operativity observed	19.7±0.7
5 min at 65 °C	–	Inhibition of LLE1 and LLE2	16.7±0.5

Table 4 Sedimentation velocity of the MCP in the presence of denaturing agents

Determination of $s_{20,w}$ values was carried out using a Centriscan 75 as described in the Experimental section.

Treatment	Concentration (M)	$s_{20,w}$ Experiment 1	Experiment 2	Experiment 3
None	–	16.0	16.8	17.2
Sodium thiocyanate	0.5	–	–	15.0
	1.0	–	14.0	–
	1.5	–	12.0	–
Urea	4.0	8.1	–	–
Guanidinium chloride	0.5	–	–	17.3
	1.5	–	–	6.0
Glycine/HCl, pH 2.3	–	3.8	–	–
Glycine/NaOH, pH 11.5	–	3.3	–	–

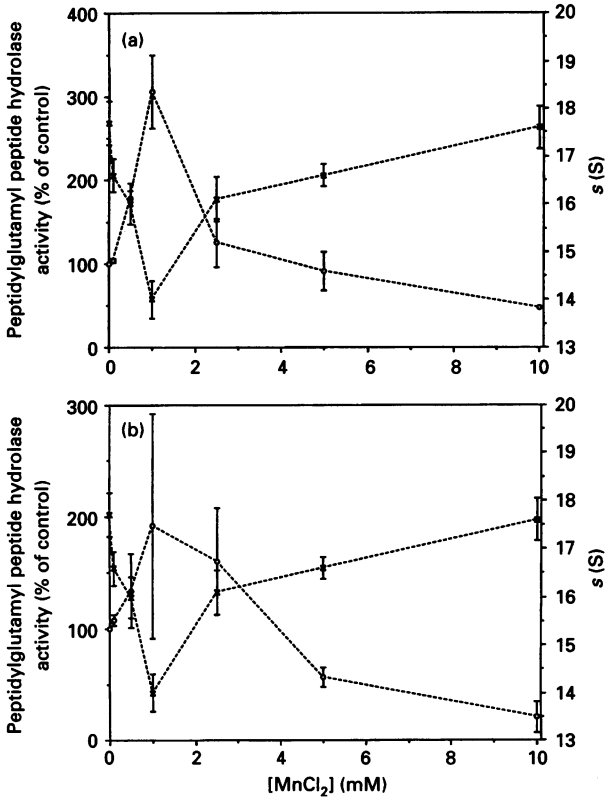

Figure 3 Dependence of the peptidylglutamylpeptide hydrolase activity and sedimentation velocity on $MnCl_2$ concentration

Hydrolysis rates of 0.1 mM (**a**) and 0.4 mM (**b**) LLE-NA were measured in 50 mM Hepes/KOH Chelex-treated buffer, 7.5, including appropriate $MnCl_2$ concentrations as described in the Experimental section (○). Determination of the $s_{20,w}$ values (×), in the presence of appropriate $MnCl_2$ concentrations, was carried out using a Beckman XLA ultracentrifuge as described in the Experimental section.

dissociation of the complex, as reflected by the low $s_{20,w}$ values (Table 4). Treatment of the complex with 4 M urea, which causes inactivation of the proteolytic activities (Rivett, 1989b), does not cause complete dissociation, as reflected by the intermediate $s_{20,w}$ value of 8.1S (Table 4). SDS/polyacrylamide gels of 4 M urea-treated MCP showed that little or no autodigestion of highly purified MCP preparations took place during a 4 h incubation on ice, although some autodigestion was apparent with higher concentrations of urea or after a longer exposure. Concentrations of 8–9 M urea were required to dissociate the complex completely (results not shown).

Under the conditions tested, MCP was found to be stable in low concentrations (< 0.5 M) of sodium thiocyanate. However, at concentrations of 1 M and higher, there was a slow loss of activity which was similar when measured with several of the synthetic peptide substrates. Treatment with 0.5, 1.0 or 1.5 M sodium thiocyanate led to a decrease in the $s_{20,w}$ value as illustrated in Table 4.

Treatment with guanidinium chloride was found to promote an activated form of the proteinase complex at concentrations below 0.05 M and to inactivate the complex at higher concentrations (Djaballah et al., 1992). The presence of 0.5 M guanidinium chloride caused little change in the $s_{20,w}$ value, whereas 1.5 M caused a reduction to 6.0S (Table 4).

DISCUSSION

Electron microscopy of negatively stained MCP preparations confirmed that the rat liver complex has a cylindrical structure similar to that of the proteinase isolated from rabbit muscle (Kopp et al., 1986; Baumeister et al., 1988) rather than the prolate ellipsoid structure with 8-fold symmetry which was proposed earlier on the basis of electron-microscopic and X-ray-scattering data(Arrigo et al., 1988; Tanaka et al., 1988a). Side-on, the proteinase appears as a stack of four rings. A hollow cylinder with a 4-fold banded structure is the simplest model compatible with the above observations. The actual structure of mammalian MCPs is likely to be more complex than the simple stacked array of four rings of six subunits each (Kopp et al., 1986). A 2-fold rotational symmetry is apparent but the optical transform suggests a pseudo-helical arrangement of subunits within the complex. This could explain the lack of true 6- or 7-fold symmetry of molecules viewed end-on as well as the discontinuities observed in the rings. This structure for mammalian MCP resembles that of the simpler archaebacterial

proteasome which is reported to be a barrel-shaped molecule possessing clear 7-fold symmetry (Dahlmann et al., 1989; Pühler et al., 1992). As pointed out by Pühler et al. (1992), the difference in structure proposed by Tanaka et al. (1988a) lies only in the interpretation of data.

The dimensions of the molecule reported here are significantly greater than those reported previously for the rat muscle proteinase (Kopp et al., 1986), but fall within the range reported for related particles (diameter 9–13 nm, height 15–20 nm; Harris, 1988; Coux et al., 1992). Particular care has been taken with calibration of the electron-microscopic magnification, and the values are valid for these preparations. In order to cross-check with a predicted solution size, r_H, the hydrodynamic radius, has been calculated. A value of r_H of 9.12 nm was obtained, which, after subtraction of two to three monolayers of water, implies a physical outer radius of about 8.7 nm for the equivalent sphere. This is in good agreement with the dimensions reported above, bearing in mind that negative staining will normally underestimate dimensions because of stain penetration. The sedimentation velocity of 17S also falls within the range of 16–22S in the literature (Harris, 1988; Tanaka et al., 1988b; Rivett, 1989a). It is clear from the data presented here that both the size of the particles and their sedimentation velocity can be significantly affected by the composition of the buffer, which may explain some of the apparent discrepancies in the literature. Moreover, it has been recognized that the size of the images observed by electron microscopy varies with the negative stain used.

Sedimentation velocity provides a convenient measure of changes in conformation associated with effectors of proteolytic activity. However, it is not possible to predict the direction of the change on the basis of a stimulatory or inhibitory effect on activity (Table 3). Activators of peptidylglutamylpeptide hydrolase activity can cause either an increase or decrease in $s_{20,w}$ value. KCl (50 mM), which inhibits LLE2 activity but has little effect on the other peptidase activities measured (Djaballah and Rivett, 1992), causes a decrease in $s_{20,w}$ value, whereas SDS can cause an increase or decrease, depending on the concentration used. Low concentrations of SDS are widely known to stimulate peptidase activities (e.g. Tanaka et al., 1990; Mykles and Haire, 1991), and changes in conformation have been suggested previously from results of fluorescence measurements (Saitoh et al., 1989). The advantages of sedimentation velocity over fluorescence measurements are that they provide a measure of both the magnitude and the direction of the change.

Sedimentation-velocity measurements of MCP in the presence of 0.4 mM LLE-NA demonstrate that an increase in $s_{20,w}$ value is associated with the positive co-operativity of the LLE2 activity (Djaballah and Rivett, 1992), suggesting a tightening of the structure. The sedimentation velocity in the presence of bivalent metal ions such as Mn^{2+}, Ca^{2+} or Mg^{2+}, which stimulate peptidylglutamylpeptide hydrolase activities (Djaballah and Rivett, 1992), is decreased, and a corresponding increase in size is detectable under the electron microscope. With $MnCl_2$ the maximum change in sedimentation velocity is observed at the concentration (1 mM) that has the maximum effect on activity. With $ZnCl_2$ and $CdCl_2$, which inhibit proteolytic activities, some aggregation was observed but there was no evidence for the dissociation by 1 mM $ZnCl_2$ reported by Scherrer and co-workers (Nothwang et al., 1992; Coux et al., 1992) for duck erythroblast prosomes.

The demonstration of conformational changes associated with selective changes in proteolytic activities of the complex suggest a possible mechanism of modulation of proteinase function *in vivo*. Although many of the agents found to stimulate activity *in vitro* are unlikely to be of significance *in vivo*, it is possible that similar conformational changes could be produced by interaction with other proteins.

This work was supported by a Medical Research Council Senior Fellowship and later by a Lister Institute–Jenner Research Fellowship awarded to A.J.R. We thank Celltech Ltd. and Professor W. V. Shaw for a studentship awarded to H.D. We also thank S. C. Hyman for help with the electron microscopy, and P. Lecane, N. Erington and P. Mistry for assistance with the hydrodynamic work.

REFERENCES

Arribas, J. and Castaño, G. (1990) J. Biol. Chem. **265**, 13969–13973
Arrigo, A.-P., Tanaka, K., Goldberg, A. L. and Welch, W. J. (1988) Nature (London) **331**, 192–194
Baumeister, W., Dahlmann, B., Hegerl, R., Kopp, F., Kuehn, L. and Pfeifer, G. (1988) FEBS Lett. **241**, 239–245
Berne, B. J. and Pecora, R. (1976) Dynamic Light Scattering, John Wiley and Sons, New York
Bowen, T. J. and Rowe, A. J. (1970) An Introduction to Ultracentrifugation, John Wiley and Sons, New York
Bradford, M. M. (1976) Anal. Biochem. **72**, 248–254
Cardozo, C., Vinitsky, A., Hidalgo, M. C., Michaud, C. and Orlowski, M. (1992) Biochemistry **31**, 7373–7380
Claes, P., Dunford, M., Kenney, A. and Vardy, P. (1992) In Laser Light Scattering in Biochemistry (Harding, S. E., Sattelle, D. B. and Bloomfield, V. A., eds.), pp. 66–76, The Royal Society of Chemistry, Cambridge
Coux, O., Nothwang, H. G., Scherrer, K., Bergsma-Schutter, W., Arnberg, A. C., Timmins, T. A., Langowski, J. and Cohen-Addad, C. (1992) FEBS Lett **300**, 49–55
Dahlmann, B., Kopp, F., Kuehn, L., Niedel, B., Pfeifer, G., Hegerl, R. and Baumeister, W. (1989) FEBS Lett. **251**, 125–131
Djaballah, H. and Rivett, A. J. (1992) Biochemistry **31**, 4133–4141
Djaballah, H., Harness, J. A., Savory, P. and Rivett, A. J. (1992) Eur. J. Biochem. **209**, 629–634
Harris, J. R. (1988) Indian J. Biochem. **25**, 459–466
Heinemeyer, W., Kleinschmidt, J. A., Saidowsky, J., Escher, C. and Wolf, D. H. (1991) EMBO J. **10**, 555–562
Kopp, F., Steiner, R., Dahlmann, B., Kuehn, L. and Reinauer, H. (1986) Biochim. Biophys. Acta **872**, 253–260
Mykles, D. L. and Haire, M. F. (1991) Arch. Biochem. Biophys. **288**, 543–551
Nothwang, H. G., Coux, O., Bey, F. and Scherrer, K. (1992) Biochem. J. **287**, 733–739
Orlowski, M. (1990) Biochemistry **29**, 10289–10297
Pühler, G., Weinkauf, S., Bachmann, L., Muller, S., Engel, A., Hergerl, R. and Baumeister, W. (1992) EMBO J. **11**, 1606–1616
Rivett, A. J. (1989a) Arch. Biochem. Biophys. **268**, 1–8
Rivett, A. J. (1989b) J. Biol. Chem. **264**, 12215–12219
Rivett, A. J. (1993) Biochem. J. **291**, 1–10
Rivett, A. J. and Sweeney, S. T. (1991) Biochem. J. **278**, 171–177
Rivett, A. J., Skilton, H. E., Rowe, A. J., Eperon, I. C. and Sweeney, S. T. (1991) Biomed. Biochim. Acta **50**, 447–450
Saitoh, Y., Yokosawa, H. and Ishii, S. (1989) Biochem. Biophys. Res. Commun. **162**, 334–339
Savory, P. J. and Rivett, A. J. (1993) Biochem. J. **289**, 45–48
Tanaka, K., Yoshimura, T., Ichihara, A., Kameyama, K. and Takagi, T. (1986) J. Biol. Chem. **261**, 15204–15207
Tanaka, K., Yoshimura, T., Ichihara, A., Ikai, A., Nishigai, M., Morimoto, Y., Sato, M., Tanaka, N., Katsube, Y., Kameyama, K. and Takagi, T. (1988a) J. Mol. Biol. **203**, 985–996
Tanaka, K., Yoshimura, T., Kumatori, A., Ichihara, A., Ikai, A., Nishigai, M., Kameyama, K. and Takagi, T. (1988b) J. Biol. Chem. **263**, 16209–16217
Tanaka, K., Yoshimura, T. and Ichihara, A. (1990) J. Biochem. (Tokyo) **106**, 495–500
van Holde, K. E. (1985) Physical Biochemistry, p. 117, Prentice Hall, Englewood Cliffs
Wilk, S. and Orlowski, M. (1983) J. Neurochem. **40**, 842–849
Yu, B., Pereira, M. and Wilk, S. (1991) J. Biol. Chem. **266**, 17396–17400

Received 2 November 1992/11 January 1993; accepted 13 January 1993